NMO stacking limitations of marine seismic data

Iverson C. M. Silva, Raimundo N. C. Carneiro, Beatriz G. Silva and Wildney W. S. Vieira*, UFOPA, UFPA*, Brazil

Abstract

The present research aimed to the procesing and imaging of marine sesismic data using the NMO methodology to construct of velocity model based in the analysis of the semblance map. Migrated sections were obtained in time and depth where it allows the interpretation.

Introduction

The main objective of seismic processing is increases the S/N ratio of data, in order to attenuate unwanted information such as noises or others interferences that can harm the final result. In this sense, in present work was aplicated the NMO methodology in seismic marine data to later imaging, using the seismic Un*x Package (Cohen and Stockwell, 2005).

The strategy was followed in this work, and resumed as 1:

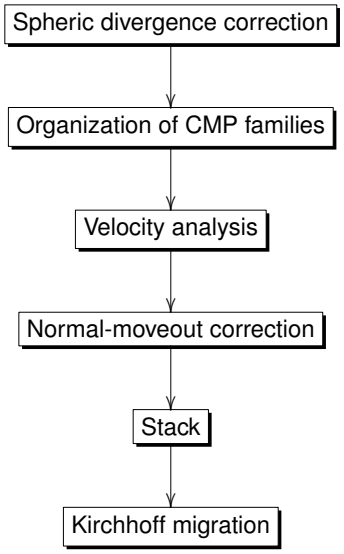

Figure 1: NMO stacking flowchart.

Acquisition parameters

The seismic data using in this procesing is the AMOCO (Dellinger et al., 2000), aquired of SEG page. The Aquisition parameters of data are shown in tabela 1

Table 1: Aquisition parameters.

Shot and receiver geometry	
shot number	385
shot interval	50 m
receiver number	256
receiver interval	25 m

CMP geometry	
CMP number	1792
CMP interval	12,5 m
maximum coverage	64

Record parameters	
Record time	3,5 s
sample interval	9,9 ms

Figure 2 shows minimum-offset data with aplication of mute before preprocessing steps.

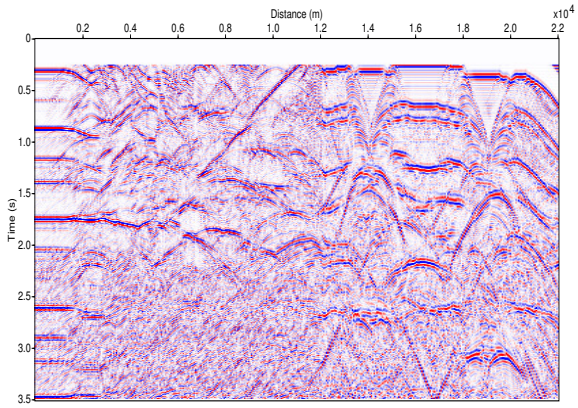

Figure 2: Minimum offset before aplication of the filters f and f-k.

Figure 3 shows he offset-minimum of data after aplication of filtering f, $f-k$ and spheric divergence correction to attenuate noises of low and righ amplitude and recover amplitudes which decay quickly.

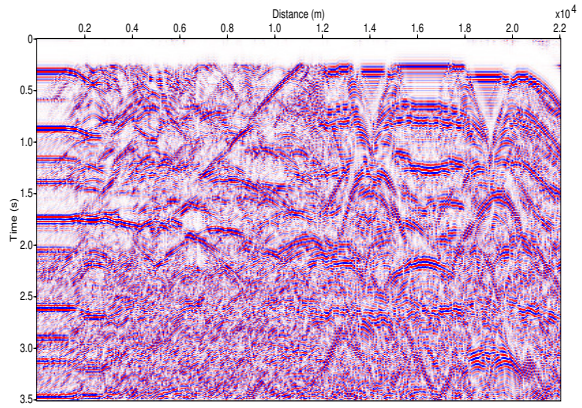

Figure 3: Minimum offset after filtering f, f-k and spheric divergen correction. It is observed sensitive increase in resolution of sesismic events.

NMO method

The methodology consisted of specific steps and organized with titles of NMO method. A commom property to these two methods is the use commom-mid-point (CMP) families, that are caracterized by the reciprocity principle source-sensor, and consequently not solving for dips. Another commom property is the semblance measure of coherence along the trajectories, $t(h)$ and $t(x_m,h)$, of the sum of traces to produce the stack CMP sections.

The beginning of this work was with the normal-moveout (NMO) correction and stack that is based on the model formed by flat, homogeneous and isotropic layers, where the transit time for the primary reflections is given by the hyperbolic approximation (1) (Hubral and Krey, 1980):

$$t(h) = \sqrt{t^2(0) + \frac{(2h)^2}{v^2}}; \qquad (1)$$

where the independent variable h is the half-offset source-receiver; $t(0)$ is the double-time relative to the normal incidence in zero offset; v is the search paramenter, where $v = v_{\text{NMO}}$ defines a velocity for the normal-moveout time correction, stack and to estimate the v_{RMS} velocity (root mean square). Therefore, this model is to be considered as initial, since it only considers vertical variation of velocity within the aperture established for the calculation. A next more complex model considers layers with dipping interfaces, but still admitting CMP families and the semblance measure.

In the NMO case, the analysis of the v parameter is performed based on the CMP family, by picking pairs of (v_{NMO}, t_0) in the semblance coherence section calculated with equation (2), where the values of $S(t_0,\mathbf{m})$ vary in the range $(0,1)$ (Sguazzero and Vesnaver, 1987):

$$S(t_0,\mathbf{m}) = \frac{1}{N} \frac{\sum_{t=t_0-\delta t/2}^{t_0+\delta t/2} \left[\sum_{h=h_1}^{h_2} \bar{u}(h,t;t_0,\mathbf{m}) \right]^2}{\sum_{t=t_0-\delta t/2}^{t_0+\delta t/2} \sum_{h=h_1}^{h_2} \left[\bar{u}(h,t;t_0,\mathbf{m}) \right]^2}, \qquad (2)$$

where $\bar{u}(h,t;t_0,\mathbf{m})$ represents the processed trace amplitude positioned along the path of the subtended sum of equation (1); N is the number of involved traces; $\mathbf{m}$ are the trajectory function parameters, $t(h;t_0,\mathbf{m})$. The sum along $t(h)$ and is defined within a spatial-temporal window where is selected a curve that best represents the reflection event. In the NMO case, the search parameter is only the velocity named $v = \mathbf{m} = v_{\text{NMO}}$ that, depending on the application, can be expressed mathematically by the v_{RMS} velocity.

Figure 4 shows the semblance map where the pairs (v_{NMO}, t_0) should be marked together with analysis of reflection events, and each event is related with one pair which better horizontaliza.

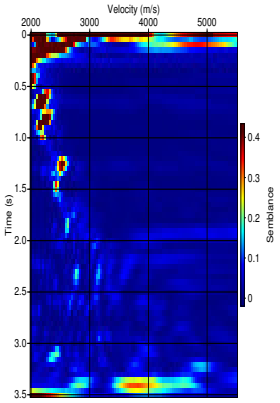

Figure 4: Semblance map for CMP 1150.

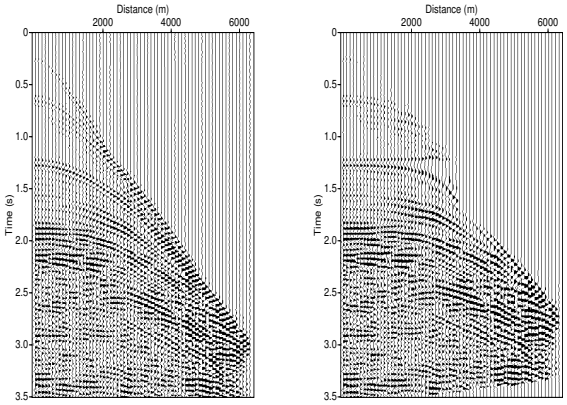

Figure 5: CMP 150 before (left), and after the NMO correction (right).

Results

Figure 6 shows the NMO velocity model time used in NMO stack.

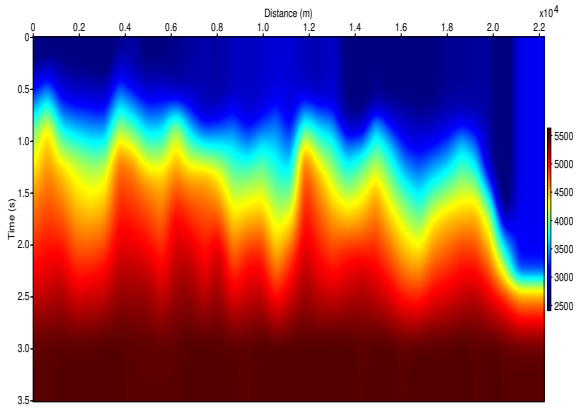

Figure 6: Velocity time model.

Stacking is done for each CMP family, which is resumed in one trace defined for:

$$\bar{s}_{t_0} = \frac{1}{N}\sum_{i=0}^{N} \bar{u}_{i,t_i}; \tag{3}$$

where $\bar{s}_{t_0}$ is the resultant amplitude of stack; $\bar{u}_{i,t_i}$ is the amplitude in i-esimo trace in double-time t_i; and N is the number of traces to be stacked in each CMP family.

Figure 7 shows the stack time data.

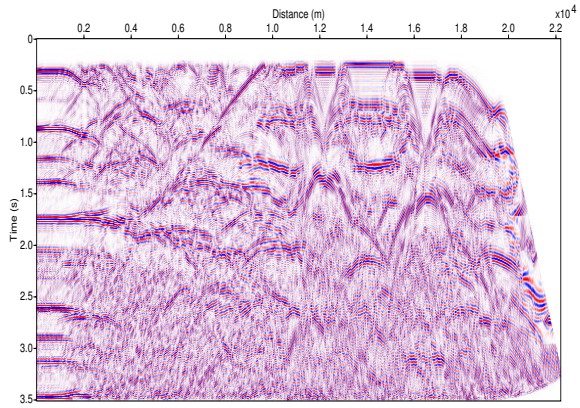

Figure 7: NMO stack in time.

Kirchhoff time migration

Migration is described from the solution of scalar wave equation without variation of density, given by:

$$\nabla^2 u(\vec{r},t) - \frac{1}{c^2}\frac{\partial^2 u(\vec{r},t)}{\partial t^2} = -4\pi q(\vec{r},t), \tag{4}$$

where $u(\vec{r},t)$ is the amplitude of field, c the velocity of medium, $q(\vec{r},t)$ the source and $\vec{r} = (x,y,z)$ point of observation.

The solution to Eq. (4) without source, considering one volume V_0 delimited for a surface S_0, is given by Grenn Theorem (Schneider, 1978):

$$u(\vec{r},t) = \frac{1}{4\pi}\int_{t_0} dt_0 \int_{S_0} dS_0 \left[G\frac{\partial}{\partial n}u(\vec{r}_0,t_0) - u(\vec{r}_0,t_0)\frac{\partial}{\partial n}G \right]; \tag{5}$$

where $\vec{n} = n\hat{n}$ is the normal vector surface S_0, which include the aquisition surface A_0, and the surface semi-spherica A' which is extrapolated for infinite so that their contribution is negligible (see Figure 8). Thus, the frontier is expressed by integral in superface of aquisition, end the solution is based in Green function which consists of response of a puntual source in $\vec{r}_0$ and its image in $\vec{r}'_0$, given by:

$$G(\vec{r},t|\vec{r}_0,t_0) = \frac{\delta\left(t - t_0 - \frac{R}{c}\right)}{R} - \frac{\delta\left(t - t_0 - \frac{R'}{c}\right)}{R'}, \tag{6}$$

onde

$$R = [(x-x_0)^2 + (y-y_0)^2 + (z-z_0)^2]^{\frac{1}{2}}, \tag{7}$$

$$R' = [(x-x_0)^2 + (y-y_0)^2 + (z+z_0)^2]^{\frac{1}{2}}. \tag{8}$$

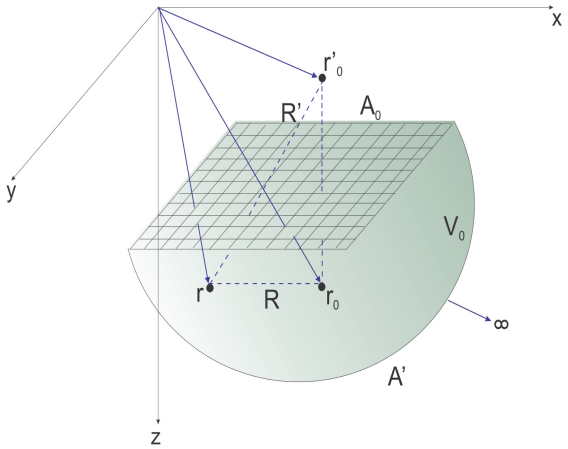

Figure 8: Scalar medium (3D) with volume V_0 delimited by the frontier $S_0 = A_0 + A'$, with one source point in $\vec{r}_0$, its image in $\vec{r}'_0$ and one observation point in $\vec{r}$ (Schneider, 1978).

The field $u(\vec{r}_0,t_0)$ is measured in frontier $S_0 = A_0 + A'$, where the Green function is canceled ($G = 0$), and the component $\frac{\partial u(\vec{r}_0,t_0)}{\partial n}$ is canceled. With this, the equation (5) is simplificated in form:

$$u(\vec{r},t) = \frac{1}{2\pi}\int_{t_0} dt_0 \int_{A_0} dA_0 \left\{ u(\vec{r}_0,t_0)\frac{\partial}{\partial z_0}\left[\frac{\delta\left(t - t_0 - \frac{R}{c}\right)}{R}\right]\right\}. \tag{9}$$

Switching $\frac{\partial}{\partial z_0}$ for $\frac{\partial}{\partial z}$ and resolving the temporal part of equation (9), it gets:

$$u(\vec{r},t) = -\frac{1}{\pi}\frac{\partial}{\partial z}\int_{A_0} dA_0 \frac{u\left(\vec{r}_0, t - \frac{R}{c}\right)}{R}. \tag{10}$$

This representation indicates which the Eq.(5) is solution of wave equation of form $\frac{f(t-\frac{R}{c})}{R}$ in integrating.

The Kirchhoff pos-stack migration in tempo was realized using the velocity model $v_{RMS}(t)$ shows in Figure 6 obtained during the velocity analysis in semblance map.

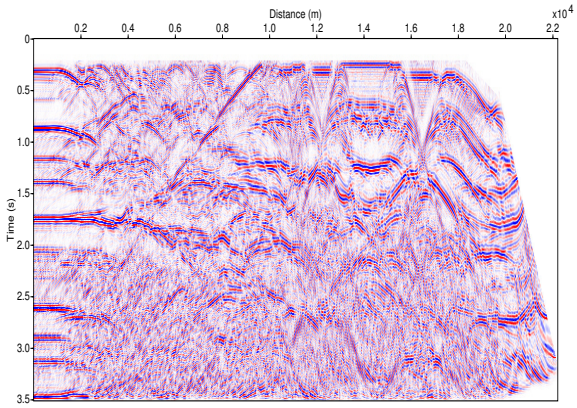

Figure 9: Kirchhoff time migration pos-stack

Analyzing this section (see Figure 9) it is noticed that the subsurface structures have not moved much in comparison the stack section shows in Figure 7. The advantages of analyzis of this migrated section is the identification of structures little perceived in stack section, and then one can observe the better continuity in the reflecting interfaces.

The velocity model in depth is obtained from the conversion of the RMS velocity to intervalar velocity and is shows in Figure 10.

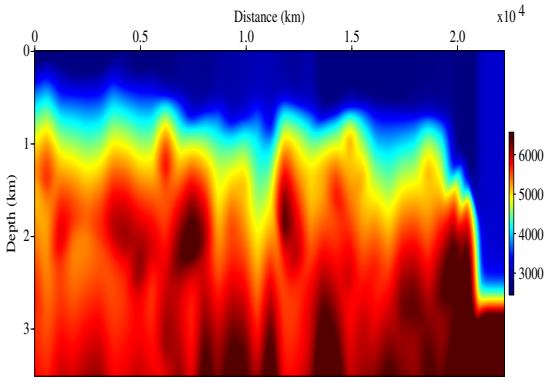

Figure 10: Velocity distribution map in depth.

The section stacked in depth is obtained from the resampling of the section stacked in time and is shows in Figure 11.

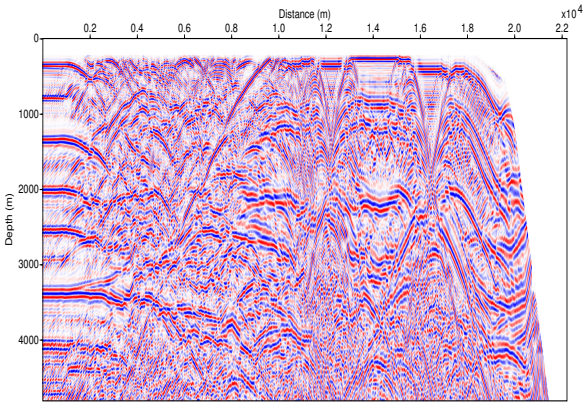

Figure 11: NMO stack in depth.

Discussion and conclusions

The conclusions on the results of the NMO stack, are clearly showing difficulties and serious limitations, as well as cases that merit further. Attention to the implementation of the theories studied, and serve as a reference for future work.

The velocity analysis was performed in the semblance map for reflection events. The obtained velocity model is presented in Figure 6, where we observe the structure of the marine data. In the stack section shown in Figure 7 we observe a meaningful increase in the S/N ratio.

A post-stack time Kirchhoff migration shown in Figure 9, that was obtained from the stack section of Figure 7, using the velocity model of Figure 6. The conclusion was for the partial collapse of some diffraction events, and the recovering of depth reflection events. But, still undesirable arc shape events are present in the deeper parts of the section. Also, a scale change of time-to-depth for the NMO stack of Figure 11. For this, it was used the interval velocity model of Figure 10 from a linear interpolation, and a constant extrapolation for points picked in the semblance map to determine the $vint(z)$ velocities for non specified time intervals. In this case the section was rescaled to 11.000 m depth.

As suggestions for future work, we propose the application of post-depth migration based on equation such as Kirchhoff, PSPI (PhaseShift Plus Interpolation), SS (Split-Step), RTM (Reverse Time Migration), and FFD (Fourier Finite Difference), for comparison with the Kirchhoff migration time, and the generalization of the results obtained with the CRS stack.

Acknowledgements

The authors would like to thank the sponsorship of Project INCT-GP, and also in special to the Project PRH-06, that are present in part of this research work. We extend our thanks also to CAPES and CNPQ for the scholarships.

References

Cohen, J. K., and Stockwell, J. J. W., 2005, Seismic un*x release n. 39: Center for Wave Phenomena, Colorado School of Mines, Colorado.

Dellinger, J. A., Gray, S. H., Murphy, G. E., and Etgen, J. T., 2000, Efficient 2.5-d true-amplitude migration: Efficient

2.5-d true-amplitude migration:, Soc. of Expl. Geophys., Geophysics, 943–950.

Hubral, P., and Krey, T., 1980, Interval velocities from seismic reflection time measurements: Society of Exploration Geophysicists, Tulsa, OK.

Schneider, W. A., 1978, Integral formulation for migration in two-dimensions and three-dimensions:, **43**, no. 01, 49–76.

Sguazzero, P., and Vesnaver, A., 1987, A comparative analysis of algorithms for stackincg velocity estimation: deconvolution and inversion: Oxford: Blackwell Scientific Publications,.